Locating of Series FACTS Devices for Multi-Objective Congestion Management Using Components of Nodal Prices

A. R. Moradi*, Y. Alinejad-Beromi*(C.A.) and K. Kiani*

Abstract: Congestion and overloading for lines are the main problems in the exploitation of power grids. The consequences of these problems in deregulated systems can be mentioned as sudden jumps in prices in some parts of the power system, lead to an increase in market power and reduction of competition in it. FACTS devices are efficient, powerful and economical tools in controlling power flows through transmission lines that play a fundamental role in congestion management. However, after removing congestion, power systems due to targeting security restrictions may be managed with a lower voltage or transient stability rather than before removing. Thus, power system stability should be considered within the construction of congestion management. In this paper, a multi-objective structure is presented for congestion management that simultaneously optimizes goals such as total operating cost, voltage and transient security. In order to achieve the desired goals, locating and sizing of series FACTS devices are done with using components of nodal prices and the newly developed grey wolf optimizer (GWO) algorithm, respectively. In order to evaluate reliability of mentioned approaches, a simulation is done on the 39-bus New England network.

Keywords: Congestion management, electricity markets, FACTS devices, multi-objective optimization, power system stability margin

1. Introduction

In deregulated environment, the process of the power grid such as generation, transmission, distribution and control are separated entities and market contributors interdepend themselves in order to sell or buy the electricity in a way to maximize their turnover. To meet the preferred transacting, power flow in the transmission system invades some of the physical restrictions of the transmission networks. Accordingly, transmission system is congested. Congestion may occur due to absent of management between generation and transmission utilities or because of unexpected probabilities likes power producer's outage, unexpected increase of load demand, or failure of equipment. The unattractive result of the congestion causes inconsistency of the system safety and increment of the power cost. Congestion can be reduced by rescheduling active power of generators, load limitation and operation of phase shifters or FACTS devices. A proper controlling action is needed effectively to mitigate the line overloads to the safety limits. There are many publications available that qualify methods for mitigating congestion in restructured power system. In [1], Ashwani Kumar et al have done a bibliographical review on congestion management systems in a competitive electricity market. The authors showed that one of the most skillful and understandable technique of congestion handling is redistributing the power outputs of generators in the system. In [2], two effective methods are suggested for solving congestion handling problem in a day ahead market by generator rescheduling. In [3], a novel ant lion optimizer has been appointed to solve the problem of congestion by redistribution of active power of generators. In [4], a new approach is suggested for palliation congestion relieving cost by feeding needed reactive power of system in addition to re-dispatching active power of generators and load shedding. A new locational marginal pricing (LMP) calculation method is suggested in [5] to deviate the main hitches with DC power flow based on LMP calculations. LMP is usually crumbled into three components, marginal cost of energy, loss and congestion which are proposed in [6]. Particle swarm optimization (PSO) is employed to solve the OPF problem in congestion management using re-dispatch of transactions in a pool market [7]. The idea of game theory in the restructured electricity market has

established communicatively to display how symmetry point of electricity market departs under the strategic gaming in [8]. The pricing of marginal transmission losses in the LMP approach in the ISO New England standard market design are presented by Litvinov et al [9]. Different calculations models and stable properties on LMP based on different market designs are propounded in [10]. A multilayer feed forward neural network is proposed for removing line overloads in real time for restructured power system [11]. In [12], the authors showed that the congestion release could be attained by re-dispatching method considering the collective operation of hydro and thermal generating companies in a deregulated environment. To solve the multi-objective optimization problem of the congestion management, a new effective multi-objective mathematical programming solution approach based on normalized normal constraint method is presented in [13]. Flexible AC Transmission System (FACTS) plays a significant role in increasing load ability and removing congestion in the network. FACTS devices can improve the efficiency extremely by controlling the power flows in the network without generation re-dispatching or structure changes [14-15]. Different approaches have been proposed for optimal location of FACTS devices including sensitivity analysis [6, 16], congestion handling by unified power flow controller (UPFC) [17] and interline power flow controller (IPFC) [18]. The authors in [19] review a fuzzy interactive multi-objective approach for the optimal location of UPFC to enhance power system operation. To manage transmission line congestion in hybrid electricity markets, the capability of Sen Transformer has been used in [20]. A PSO-based algorithm is used to find the optimal position and the parameters setting of UPFC to increase load ability [21]. In [22], it reviews a fuzzy-genetic algorithm (GA) approach for the optimal placement of FACTS devices in a power system for congestion management. A GA-based algorithm is used in [23] to find the optimal locating and the parameters setting of Thyristor Controlled Series Compensator (TCSC) to increase loadability. In [24], the TCSC are located for congestion management in the power system by considering the non-smooth fuel cost function and penalty cost of emission. In this reference, bacterial foraging and Nelder-Mead algorithm is applied to solve TCSC placement problem for congestion management.

None of the mentioned references has considered power system security concerns. Thus, power system stability should be considered within the construction of congestion management. On the other hand, in order to improve power system security, significant references are presented to apply FACTS devices. In [25], trajectory sensitivity approach for optimal locating of series FACTS devices is presented to enhance transient stability. To maintain the voltage stability in the power transmission system, a novel technique is presented in [26], to optimize the FACTS devices. In this reference, the PSO and the adaptive gravitational search algorithm (GSA) technique are presented for improving the voltage stability of the power transmission systems.

In this paper, a multi-objective structure is presented for congestion management that simultaneously optimizes goals such as total operating cost, voltage and transient security. Voltage Stability Margin (VSM) [27] and Corrected Transient Energy Margin (CTEM) [28] indices are applied in this paper for measuring of voltage and transient security margins, respectively. In order to achieve the desired goals, locating and sizing of series FACTS devices (TCSC is considered as a series FACTS device) are done via using the components of nodal prices and the newly developed grey wolf optimizer (GWO) algorithm, respectively.

Most of the references use methods based on the iteration for optimal locating of FACTS devices. These methods may not achieve optimal solution and they consume lots of time. Therefore, for solving these challenges, this paper tries to indicate a new methodology to locate the best position of FACTS devices for congestion management in the deregulated electricity markets. Also, this method indicates the accuracy explanation of each nodal price, by categorizing each nodal price into variety of elements corresponding to the important factors, as generations, transmission density, voltage constraints and other limitations. The decomposition is unique and components in each nodal price are identical to increase the values from the economic criteria by utilizing of derivations that are based on the marginal conditions. This full information for nodal prices can be used not only to improve the efficient usage of power grid and congestion management, but also this information tries to design a suitable pricing structure of power systems, to prepare economic signals for generation or transmission investment. The proposed method is applicable to any type of series FACTS devices.

On the other hand, a new algorithm based on the swarm intelligence named as GWO for sizing of TCSC has been used. This algorithm is inspired by the social behavior of grey wolves in nature. It can be expressed that the GWO algorithm has a better convergence in contrast with the other algorithms that are similar because of employing the same mathematical model in order to search optimal solutions. It should be mentioned that GWO algorithm check the search space with high speed in the initial steps for finding the optimal solution then by reaching the final steps, it reduces speed of changing position. So, convergence of an algorithm is guaranteed in the search space. The efficiency of these methods is performed with 39-bus New England system.

Structure of the article is as follows: 2th chapter presents the mathematical model of TCSC. Derivation of nodal price is in 3th chapter. 4th chapter describes the pro-

posed placement methodology for series FACTS devices in deregulated market. 5th, 6th chapters are simulation results and conclusion, respectively.

2. Modelling of TCSC

The transmission line model with a TCSC joint between the two buses i and j is shown in Fig. 1. TCSC can be considered as a static reactance of magnitude equivalent to -jX_C. The controllable reactance is directly used as a control variable to be implemented in power flow equation.

The variation in the line flow because of series capacitance can be illustrated as a line without series capacitance with power injected at the both ends of the line in sending and receiving as shown in Fig. 2.

The active and reactive power infusions due to TCSC at bus-i and bus-j can be expressed as,

$$P_{ic} = V_i^2 \Delta G_{ij} - V_i V_j [\Delta G_{ij} \cos(\delta_i - \delta_j) + \Delta B_{ij} \sin(\delta_i - \delta_j)] \tag{1}$$

$$P_{jc} = V_j^2 \Delta G_{ij} - V_i V_j [\Delta G_{ij} \cos(\delta_i - \delta_j) - \Delta B_{ij} \sin(\delta_i - \delta_j)] \tag{2}$$

$$Q_{ic} = -V_i^2 \Delta B_{ij} - V_i V_j [\Delta G_{ij} \sin(\delta_i - \delta_j) - \Delta B_{ij} \cos(\delta_i - \delta_j)] \tag{3}$$

$$Q_{jc} = -V_j^2 \Delta B_{ij} + V_i V_j [\Delta G_{ij} \sin(\delta_i - \delta_j) + \Delta B_{ij} \cos(\delta_i - \delta_j)] \tag{4}$$
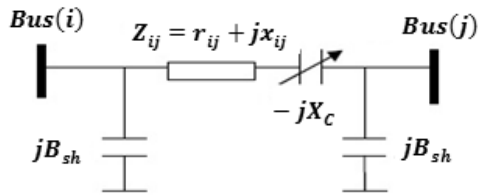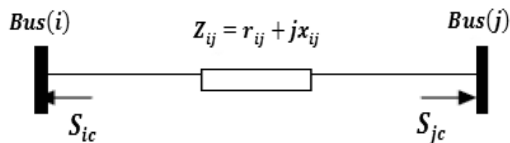

Fig. 1. Model of Transmission line with TCSC

Fig. 2. Injection model of TCSC

where

$$\Delta G_{ij} = \frac{r_{ij} x_c (x_c - 2x_{ij})}{[r_{ij}^2 + (x_{ij} - x_c)^2](r_{ij}^2 + x_{ij}^2)} \tag{5}$$

$$\Delta B_{ij} = \frac{-x_c (r_{ij}^2 - x_{ij}^2 + x_{ij} x_c)}{[r_{ij}^2 + (x_{ij} - x_c)^2](r_{ij}^2 + x_{ij}^2)} \tag{6}$$

This model of TCSC is applied to properly change the parameters of transmission line with TCSC for optimal location.

3. Extraction of nodal price
3.1 Problem formulation

In this paper, a multi-objective congestion management structure is formulated to determine the optimal locating and sizing of TCSC. The proposed structure minimizes the total operating cost and maximizes voltage stability margin (VSM) and corrected transient energy margin (CTEM) to enhance the stability of the power system. The phrases for these goals are given as follows:

- Minimize f1: Total operating cost

$$\text{Minimize } f_1 = \left(\sum_{k \in SG} C_{Gk}(P_{Gk}) - \sum_{k \in SD} B_{Dk}(P_{Dk}) \right) \tag{7}$$

where SD and SG are the set of participating demands and generators in the market, respectively. Also B_Dk and C_Gk are the benefit curve of kth demand and bid curve of kth generator, respectively. It is noteworthy that the benefit curve of demands and bid curve of generators are considered as quadratic functions [29].

- Maximize f_2: Voltage stability margin (VSM)

In this paper, VSM [27] is the index used for measuring voltage security and continuation power flow (CPF) is used to define the maximum load ability limit.

After using congestion management, the final VSM is given below:

$$\text{Maximize } f_2 = VSM = VSM_0 + \Delta VSM \tag{8}$$

where VSM_0 is the VSM value before using congestion management and the phrase for ΔVSM is given as follows [30]:

$$\Delta VSM \cong -\frac{\partial VSM}{\partial Q_{Di}}Q_{ic} - \frac{\partial VSM}{\partial Q_{Dj}}Q_{jc}$$
$$+ \sum_{k \in SD} \frac{\partial VSM}{\partial Q_{Dk}}\Delta Q_{Dk} \tag{9}$$

where i and j are the two buses of the branch where the TCSC is installed. Q_ic and Q_jc are reactive powers injected to buses because of installing TCSC as shown in Fig. 2. Q_Dk is reactive power consumption of kth demand and SD is the set of participating demands in the market.

- Maximize f3: Corrected transient energy margin (CTEM)

In this paper, CTEM [28] is the index used to measure transient security. CTEM is defined as a function of generators' active power generation.

After using congestion management, the final CTEM is given as follows:

$$\text{Maximize } f_3 = CTEM = CTEM_0 + \Delta CTEM \tag{10}$$

where $CTEM_0$ is the CTEM value before using congestion management and the phrase for $\Delta CTEM$ is given as follows [30]:

$$\Delta CTEM \cong \sum_{k \in SG} \frac{\partial CTEM}{\partial P_{Gk}}\Delta P_{Gk} \tag{11}$$

where P_{Gk} is active power production of kth generator and SG is the set of participating generators in the market.

The optimization is performed under the following equality and inequality constraints:

- Equality constraints:
   a) Power balance equation

$$P_i(\theta, V) - P_{Gi} + P_{Di} = 0, \quad \text{for any node } i, \tag{12}$$

$$Q_i(\theta, V) - Q_{Gi} + Q_{Di} = 0, \quad \text{for any node } i, \tag{13}$$

If TCSC is located in line between buses i and j, the power balance equations in nodes i and j are given by:

$$P_i(\theta, V) - P_{Gi} + P_{Di} + P_{ic} = 0, \quad \text{for any node } i, \tag{14}$$

$$Q_i(\theta, V) - Q_{Gi} + Q_{Di} + Q_{ic} = 0, \quad \text{for any node } i, \tag{15}$$

$$P_j(\theta, V) - P_{Gj} + P_{Dj} + P_{jc} = 0, \quad \text{for any node } j, \tag{16}$$

$$Q_j(\theta, V) - Q_{Gj} + Q_{Dj} + Q_{jc} = 0, \quad \text{for any node } j, \tag{17}$$

where P_{Gi} and Q_{Gi} are active and reactive power production at bus i, P_{Di} and Q_{Di} are active and reactive power consumption at bus i, P_{ic} and Q_{ic} are the net active and reactive power injection at bus i.

- Inequality constraints:
   a) Apparent line flow limit

$$|S_{ij}(\theta, V)| \leq S_{ij}^{max} \tag{18}$$

   b) Power generation limit

$$P_{Gi}^{min} \leq P_{Gi} \leq P_{Gi}^{max} \tag{19}$$

$$Q_{Gi}^{min} \leq Q_{Gi} \leq Q_{Gi}^{max} \tag{20}$$

   c) Demand limit

$$P_{Di}^{min} \leq P_{Di} \leq P_{Di}^{max} \tag{21}$$

$$P_{Di}^{min} \leq P_{Di} \leq P_{Di}^{max} \tag{22}$$

   d) Bus voltage limit

$$V_i^{min} \leq V_i \leq V_i^{max} \tag{23}$$

   e) TCSC reactance limit

$$x_c^{min} \leq x_c \leq x_c^{max} \tag{24}$$

   f) VSM limit

$$VSM \geq VSM_0 \tag{25}$$

   g) CTEM limit

$$CTEM \geq CTEM_0 \tag{26}$$

where P_{Gi}^{min} and P_{Gi}^{max} are minimum and maximum active power production at bus i, Q_{Gi}^{min} and Q_{Gi}^{max} are minimum and maximum reactive power production at bus i, P_{Di}^{min} and P_{Di}^{max} are minimum and maximum active power consumption at bus i, Q_{Di}^{min} and Q_{Di}^{max} are minimum and maximum reactive power consumption at bus i, V_i^{min} and V_i^{max} are minimum and maximum voltage at bus i, S_{ij} is the apparent power in transmission line connecting buses i and j, and S_{ij}^{max} is its maximum limit, x_c^{min} and x_c^{max} are the minimum and maximum limits of TCSC reactance, and N is the number of buses in the system.

3.2 Nodal price

Define the Lagrangian function as L, then

$$L(X,\lambda,\rho,P,Q) = f(X,P,Q) + \lambda\, G(X,P,Q) + \rho\, H(X,P,Q) \quad (27)$$

where $\lambda = (\lambda_1, \ldots, \lambda_{n1})$ and $\rho = (\rho_1, \ldots, \rho_{n2})$ are the lagrangian multipliers associated with equality and inequality constraints, respectively, in addition to it they are usually explained as shadow prices from the economics point of view.

Then at an optimal solution (X, λ, ρ) and for a set of given (P, Q), the nodal prices of real and reactive power for each bus are presented for $k = 1,\ldots, n$ as follows:

$$\pi_{P,k} = \frac{\partial L}{\partial P_k} = \frac{\partial f}{\partial P_k} + \lambda \frac{\partial G}{\partial P_k} + \rho \frac{\partial H}{\partial P_k} \quad (28)$$

$$\pi_{q,k} = \frac{\partial L}{\partial q_k} = \frac{\partial f}{\partial q_k} + \lambda \frac{\partial G}{\partial q_k} + \rho \frac{\partial H}{\partial q_k} \quad (29)$$

A remarkable trait for nodal prices is that each nodal price is absolutely defined simply as a linear summation of all factors according to Eq. (28) and (29) equation because each nodal price, e.g., $\pi_{(P,k)}$ can be rewritten as,

$$\pi_{P,k} = \sum_i \frac{\partial f_i}{\partial P_k} + \sum_i \lambda_i \frac{\partial g_i}{\partial P_k} + \sum_i \rho_i \frac{\partial h_i}{\partial P_k} \quad (30)$$

On the other hand, this trait is completely different from that of AC load flow, which is generally nonlinear to each route or source. Therefore, theoretically it is possible to trace the contributions of all factors engaging in performance of power systems to each nodal price.

4. Proposed methodology

There are numerous constraints or factors affecting the operation of power systems, e.g., line flow limitation, generators, voltage limitation, and power flow balance situation. Some of them (e.g., voltage constraint) have market values that may be relaxed and taken as some tradable things rely on market needs. The relaxation for these limits may be figured out by facility investments or technology innovations, etc. However, some of them really cannot be traded, e.g., for real power flow balance situation at each bus, the summation of all injected real power at each bus must be zero which cannot be relaxed or violated because it is a physical law. However, the evaluation for the factors with no market value is pointless, even though we can theoretically follow the shares of all factors involving in the performances of power systems to each nodal price. Hence, before breaking down the nodal prices, we have to classify all constraints in the performances of power systems into two groups [31], i.e., no tradable constraints that are forcible constraints during the operation and are not components of nodal prices, and tradable constraints, which should be components of each nodal price. Let M be the constraints which we do not intend expressly to count their charges for nodal prices (no tradable constraints), and N be the remaining constraints (tradable constraints). Define α to be the Lagrangian multipliers corresponding to the constraints of M, and β to be the remaining Lagrangian multipliers corresponding to N.

By considering X and α as functions of (P, Q), the Lagrangian function of Eq. (27) can be rewritten as follows [31]:

$$
\begin{aligned}
&L(X(P,Q), \alpha(P,Q), P, Q) \\
&= f(X(P,Q), P, Q) + \alpha(P,Q)M(X(P,Q), P, Q) \\
&+ \beta N(X(P,Q), P, Q)
\end{aligned} \quad (31)
$$

Therefore, differentiating L of Eq. (31) with respect to p_k and q_k, nodal prices of Eq. (28) and (29) become,

$$\pi_{p,k} = \left(f_X X_{pk} + f_{pk}\right) + \beta\left(N_X X_{pk} + N_{pk}\right) \quad (32)$$

$$\pi_{q,k} = \left(f_X X_{qk} + f_{qk}\right) + \beta\left(N_X X_{qk} + N_{qk}\right)$$
$$(k = 1, \ldots, n) \quad (33)$$

Next, we display that Eq. (32) is actually the decomposed nodal prices. If the objective function is constructed by many factors, i.e., $f=\sum_i f_i$, then $f_X X_{pk}+f_{pk}=\sum_i((\partial f_i/\partial x)(\partial x/\partial_{pk})+(\partial f_i/\partial pk))$ for the first term of Eq. (32). Let $N=(N_1, N_2, \ldots)^T$ and $\beta=(\beta_1, \beta_2, \ldots)$ where N_j and β_j are the jth equation of N and its respective lagrangian multiplier. Then the second term of Eq. (32) can be represented as $\beta(N_X X_{pk}+N_{pk})=\sum_J \beta j((\partial N_j/\partial x)(\partial x/\partial_{pk})+(\partial N_j/\partial pk))$. Therefore, $((\partial f_i/\partial x)(\partial x/\partial_{pk})+(\partial f_i/\partial pk))$ is the component associated to the factor f_i (e.g., the ith generator) for real power, while $\beta j((\partial N_j/\partial x)(\partial x/\partial_{P_k})+(\partial N_j/\partial pk))$ represent the term of the respective constraint N_j for real power. Generally, each term in Eq. (32) is nonzero at an optimal solution, in contrast with the terms of Eq. (28).

5. Simulation results and discussion

Because of the high cost of power flow control devices installation and variety of these devices and also changing the price of these devices with changing capacity, the system operator should study carefully in order to select type, capacity and a good place to install these devices. Economical installation costs of FACTS devices in the network should be checked from the point of view of consumer, producer and operator. It is very important economically and it has tried to check the subject in order to analyze the impact of devices on the network to obtain properly analysis.

In this paper, for 39-bus New England system which is shown in Fig. 3, four scenarios have been described according to Table 1 that shows minimum and maximum demand of spring and summer seasons. To simulate congestion, these scenarios have been considered as increment factor (λ) and multiply in all system loads. To calculate the amount of power flow on each line, buses voltage, active and reactive power generation of power plants, consumption of active and reactive power of load buses and other values, optimal power flow (OPF) for each scenario has been performed. Then, component of nodal price method indicates the accuracy for explanation of each nodal price, by categorizing each nodal price into variety of elements corresponding to the important factors, as generations, transmission density, voltage constraints and other limitations. After performing OPF in all scenarios, each nodal price is checked to find impact of activated constraint in network on each bus price. By calculating component of nodal price, enough information for the analysis of prices and deciding on the allocation of devices is obtained.

In this paper, to manage congestion, dense lines in different scenarios are separated from another line and then the most effective dense line that has more effect on nodal prices is selected. This means that because of rising demand in the system, number of dense lines in the system is increased too, and because it is not possible to install FACTS devices in several lines due to more cost of installation, the system operator must choose most effective line between the all dense lines. Therefore, the importance of the allocation of the power flow control devices to control density on the network is increased.

5. 1. Analysis of network in the presence of congestion of transmission lines

Table 2 shows the results after implementing optimal power flow for four scenarios in 39-bus New England system. In this paper, the capacity of lines 1-2, 6-7, 12-11 and
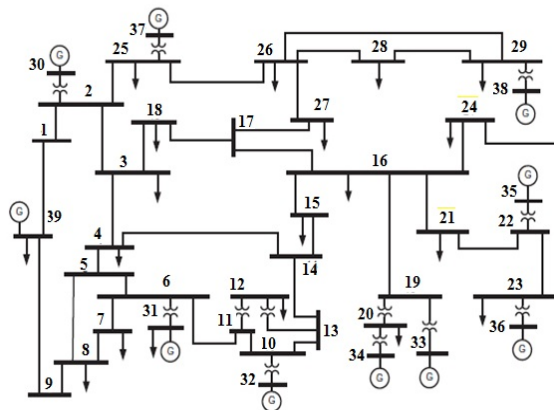
Table 1. Scenarios defined

		λ = Load Level
Spring	Scenario1	0.3
	Scenario2	1
Summer	Scenario3	0.8
	Scenario4	1.023

Table 2. Active constraints in each scenario

Scenario 1	congested line number 1 , from 1 to 2 congested line number 21 , from 11 to 12 voltage amplitude constraint (V) at bus 25 voltage amplitude constraint (V) at bus 31 reactive power constraint (Q) at genco 1 reactive power constraint (Q) at genco 8
Scenario 2	congested line number 3 , from 2 to 3 congested line number 12 , from 6 to 7 congested line number 31 , from 17 to 27 congested line number 21 , from 11 to 12 voltage amplitude constraint (V) at bus 19 voltage amplitude constraint (V) at bus 22 voltage amplitude constraint (V) at bus 25 voltage amplitude constraint (V) at bus 31 voltage amplitude constraint (V) at bus 35 voltage amplitude constraint (V) at bus 36 active power constraint (P) at genco 5 reactive power constraint (Q) at genco 1 reactive power constraint (Q) at genco 3 reactive power constraint (Q) at genco 8
Scenario 3	congested line number 1 , from 1 to 2 congested line number 12 , from 6 to 7 congested line number 31 , from 17 to 27 congested line number 21 , from 11 to 12 voltage amplitude constraint (V) at bus 19 voltage amplitude constraint (V) at bus 22 voltage amplitude constraint (V) at bus 25 voltage amplitude constraint (V) at bus 31 voltage amplitude constraint (V) at bus 36 reactive power constraint (Q) at genco 8
Scenario 4	congested line number 1 , from 1 to 2 congested line number 12 , from 6 to 7 congested line number 3 , from 2 to 3 congested line number 21 , from 11 to 12 voltage amplitude constraint (V) at bus 19 voltage amplitude constraint (V) at bus 25 voltage amplitude constraint (V) at bus 26 voltage amplitude constraint (V) at bus 28 voltage amplitude constraint (V) at bus 29 voltage amplitude constraint (V) at bus 31 voltage amplitude constraint (V) at bus 35 voltage amplitude constraint (V) at bus 36 active power constraint (P) at genco 4 active power constraint (P) at genco 5 active power constraint (P) at genco 10 reactive power constraint (Q) at genco 1 reactive power constraint (Q) at genco 3 reactive power constraint (Q) at genco 8

17-27 are set to 150, 330, 40 and 50 MVA, respectively, as extra suppositions [30].

Checking the activated constraints in four scenarios show that by changing the load levels in the system, limitations would occur that these limitations include approaching plants generation to the highest and lowest level of their generation. In both cases, this limitation has impact on the network power flow and the price of buses. Another limitation is the voltage level of buses. As it is known, the voltage level must be provided in a specified

Fig. 3. 39-bus New England system

tolerance for the consumer because power systems equipment and consumer equipment would be damaged when voltage level achieves to high or low level. Also, these limitations make problems in the network that are compromised by the stability of the power system, so they must be removed. The final limitation is overloading of transmission lines that the importance of this constraint in the power network is great. Since the transmission lines are connector between the producer and consumer, and since the amount of consumption in network is increased daily and new consumer feed from this system, power system operator must create a competitive market that all participants can access to network easily and freely.

In addition, by checking activated constraints in all scenarios, congestion limitation of transmission lines is separated from another limitation. It should be mentioned that the most important criteria for choosing the line is the impact of this on buses price and the number of congestion in different scenarios. According to the mentioned criteria, candidate transmission lines for installation of TCSC in 39-bus New England system are given in Table 3.

Also, In order to evaluate dependability of the proposed method, the results of simulation with LMP differences method [6] for optimal locating of TCSC are added to Table 3.

The results show that, the proposed method determines the lines 21, 12, 1, 3 and 31 as the candidate locations for the installation of TCSC, respectively. In contrast, the LMP different method determines the lines 12, 1, 11, 10 and 6 as the candidate locations for the installation of TCSC based on minimum total congestion cost, respectively. It can be seen that the lines 12 and 1 in both methods are repeated.

Furthermore, proposed method is a competitive tool to determine the optimal location of FACTS devices. In this paper, the line 12 is considered as the best location for the installation of TCSC.

5. 2. Sizing TCSC using MOGWO algorithm
5.2.1 MOGWO

This section summarizes the main steps in multi objective grey wolf optimizer (MOGWO) algorithm. The

Table 3. Candidate branches for TCSC in 39-bus New England system

Candidate numbers	Proposed method	LMP differences method [6]
	Candidate locations	Candidate locations
1	Line 21: 11-12	Line 12: 6-7
2	Line 12: 6-7	Line 1: 1-2
3	Line 1: 1-2	Line 11: 5-8
4	Line 3: 2-3	Line 10: 5-6
5	Line 31: 17-27	Line 6: 3-4

GWO is a new meta-heuristic algorithm inspired by grey wolves. The GWO algorithm mimics the hunting mechanism and headship hierarchy of grey wolves in nature. Four kinds of grey wolves such as alpha, beta, delta, and omega are used for simulating the leadership hierarchy. Also, three main steps of hunting, entitled seeking for hunt, encircling hunt, and attacking to hunt are accomplished.

For mathematical social hierarchy modeling of grey wolf, it is assumed that the best solutions are obtained by the wolves, alpha (α), beta (β) and delta (δ), respectively and other wolves are assumed to be omega (ω). In fact, hunting would be guided by three wolves, alpha, beta and delta and other wolves follow these three wolves.

Encircling prey can be modeled by the following equations:

$$\vec{D} = \left| \vec{C}.\vec{X}_p(i) - \vec{X}(i) \right| \tag{34}$$

$$\vec{X}(i + 1) = \vec{X}_p(i) - \vec{A}.\vec{D} \tag{35}$$

where i is the present iteration, $\vec{C}$ and $\vec{A}$ are coefficient vectors, $\vec{(X_p)}$ represents the position vector of the victim, and $\vec{X}$ represents the position vector of a grey wolf.

The vectors $\vec{A}$ and $\vec{C}$ are calculated from the following equations:

$$\vec{A} = 2\vec{a}.\vec{r}_1 - \vec{a} \tag{36}$$

$$\vec{C} = 2.\vec{r}_2 \tag{37}$$

In Eq. (36) and (37), coefficient $\vec{a}$ decreases linearly from 2 to 0 in each iteration and $\vec{r}_1$ and $\vec{r}_2$ are random vectors between [0, 1].

For mathematical modeling of hunting, it is assumed that α is the best answer and β, δ are best knowledge for prey position. With saving these three answers and updating other search agents such as ω by the following equations, the new answers may be achieved. This continues up to reaching the best answers. In this algorithm, for searching a prey, grey wolves diverge from each other. Mathematically modeling, when $|\vec{A}|>1$ forces the wolves to diverge from wide search space, hopefully find a better position. Afterwards estimating a prey converge they would get ready to raid the prey. Also, $(\vec{C})$ vector component has random values between [0-2] that not linearly decrease in contrast to $(\vec{A})$. This parameter helps to avoid algorithm of stopping on local optimum.

$$\vec{D}_\alpha = \left| \vec{C}_1.\vec{X}_\alpha - \vec{X} \right|, \vec{D}_\beta = \left| \vec{C}_2.\vec{X}_\beta - \vec{X} \right|, \vec{D}_\delta = \left| \vec{C}_3.\vec{X}_\delta - \vec{X} \right| \tag{38}$$

$$\vec{X}_1 = \vec{X}_\alpha - \vec{A}_1.\left(\vec{D}_\alpha\right) , \vec{X}_2 = \vec{X}_\beta - \vec{A}_2.\left(\vec{D}_\beta\right) , \vec{X}_3 = \vec{X}_\delta - \vec{A}_3.\left(\vec{D}_\delta\right) \qquad (39)$$

$$\vec{X}(i+1) = \frac{\vec{X}_1 + \vec{X}_2 + \vec{X}_3}{3} \qquad (40)$$

Fig. 4 shows that in a two-dimensional space, how the search agents are updated by alpha, beta and delta positions. In other words, Fig. 4 shows that α, β and δ estimate probable position of the prey (best answer) in the search space and other wolves update their position in the random place within a circle around the α, β and δ.

Two new components: first, an archive that is responsible for storage of optimal solutions of non-dominated Pareto and second, leader selection strategy that helps to choose the best leader between archive, are added here in order to create multi objective GWO algorithm [32]. Auxiliary components added are similar to MOPSO method. An archive that is added for creating multi objective GWO algorithm is a simple storage unit. This unit stores the best optimal solutions of non-dominated Pareto obtained so far.

The second component helps us choose the leader by using roulette wheel method and probability function that is introduced in the following:

$$p_i = \frac{C1}{N_i} \qquad (41)$$

C1: a constant number greater than 1

N_i: Number of obtained Pareto optimal solutions in the ith segment.

More comprehensive description of the MOGWO algorithm is given in [32].

5.2.2 Utilization of MOGWO in sizing TCSC

In this section, the MOGWO algorithm for sizing of TCSC is presented. In this algorithm, first, initial population of wolves, parameter $\vec{a}$, coefficient vectors($\vec{A}$), $\vec{C}$ and maximum numbers of iteration are defined. Then, initial population of wolves are spread randomly in the defined search space that the position of each wolf has been considered as value of TCSC. For each position, optimal power flow runs in order to calculate the fitness functions according to equations (7), (8), and (10), subject to satisfy constraints (12) to (26). Then, the non-dominant solutions are determined and the archive is initialized according to them. The best position of wolves in the archive, are named as α, β and δ and the position of the rest of wolves are called ω. Then, the value of parameter $\vec{a}$ decreases linearly from 2 to 0 in each iteration in order to confirm exploration and exploitation.

At this point, the position of the other wolves (ω) relative to top wolves' position (alpha, beta and delta), is updated according to equations (38) and (39). This update, takes places according to distance of rest of the wolves (ω) from top wolves' position (alpha, beta and delta) and are named as X_1, X_2 and X_3. Then, next new position is obtained by calculating average of the positions X_1, X_2 and X_3 according to equation (40). The value of fitness functions for this position is calculated. At this time, the non-dominant solutions are determined and the archive is updated according to them. Then if the archive would be full, the grid mechanism runs to omit one of the current archive members and add the new solution to the archive.
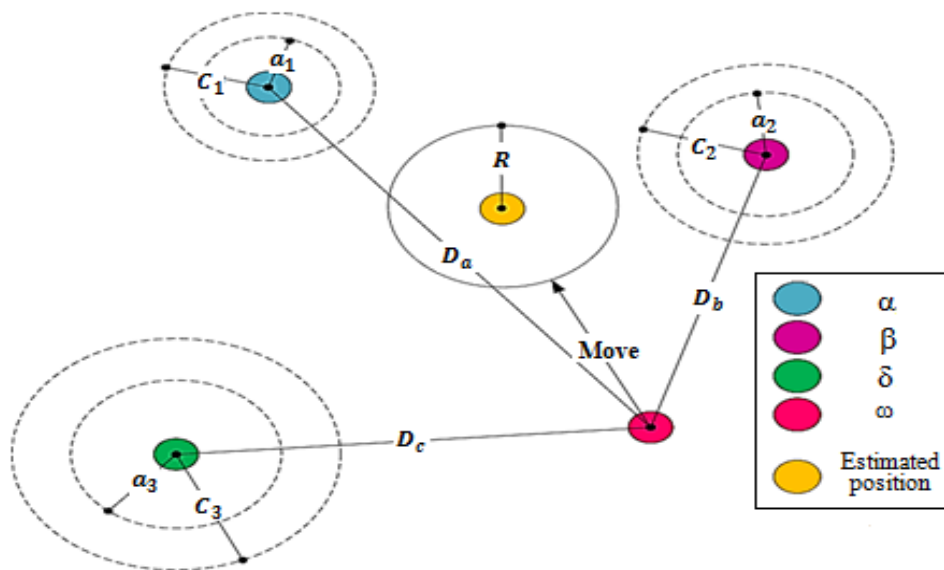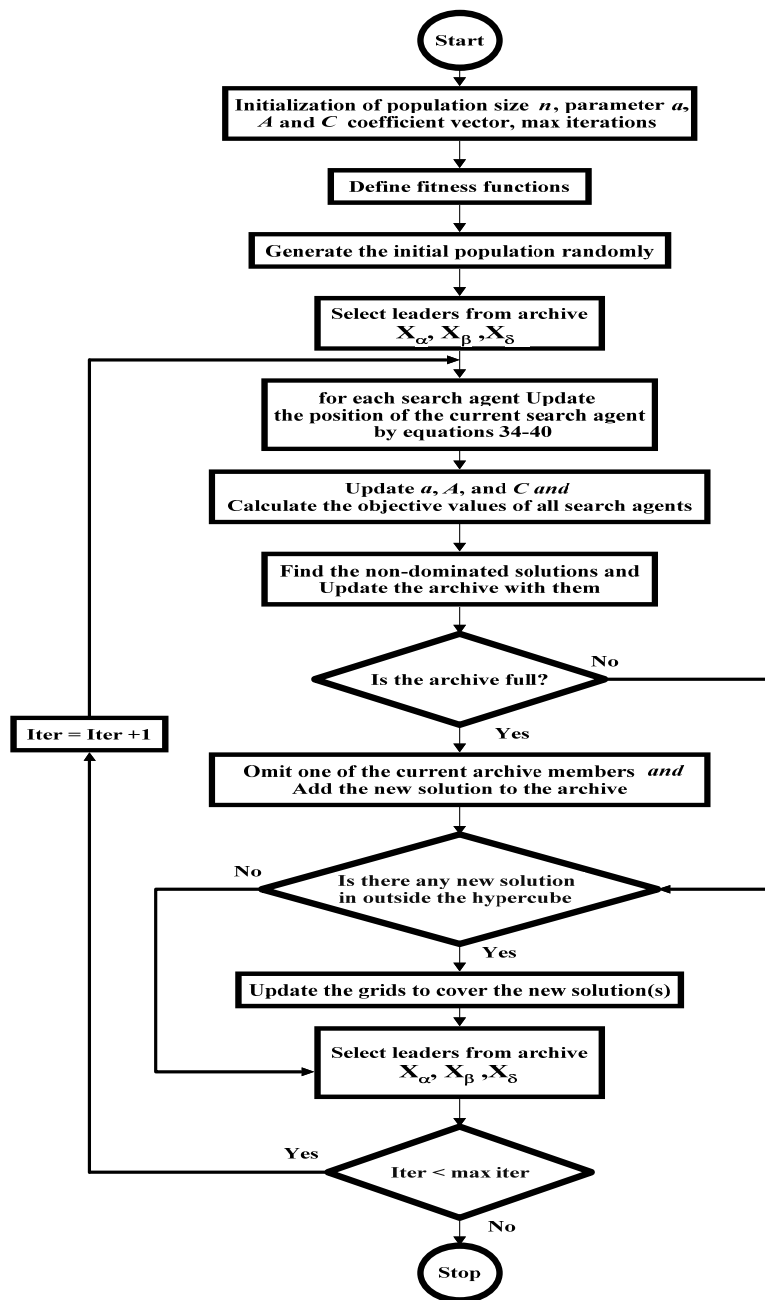

Fig. 4. Position updating in GWO

Fig. 5. The flowchart of utilization of MOGWO algorithm in sizing TCSC

Else, if each of the new added solutions to the archive is located outside the hypercube, update the grids to cover the new solution(s). Else, select leaders from the archive. These processes will be continued until reaching favorable position or maximum iteration. The flowchart of utilization of MOGWO algorithm in sizing TCSC is shown in Fig. 5.

5. 3. Fuzzy method

In order to specify a set of solutions, we need to get a pliable solution and demonstrate a trade-off among various objectives. In case of selecting an agreed-upon solution among a set of solutions, there are different approaches. A fuzzy method is of great interest because of its ease. The fuzzy sets are specified by membership functions that represent the grade of membership in a fuzzy set, with values from 0 to 1 [33]. In the fuzzy ap-
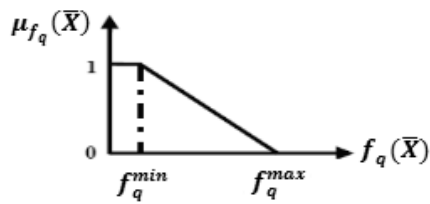
Fig. 6. Linear type membership function

proach, a strictly monotonically decreasing and continuous membership function is defined for each objective.

The membership function illustrates the extent in which a solution is satisfying the objective functions q. A linear membership function can be applied for all objectives:

$$\mu_{f_q}(\bar{X}) = \begin{cases} 0 & f_q(\bar{X}) > f_q^{max} \\ \frac{f_q^{max} - f_q(\bar{X})}{f_q^{max} - f_q^{min}} & f_q^{min} \le f_q(\bar{X}) \le f_q^{max} \\ 1 & f_q(\bar{X}) < f_q^{min} \end{cases} \quad (42)$$

Fig. 6 shows the graph of this membership function.

By taking the individual minimum and maximum values of each objective function into account, the membership function $\mu_{(f_q)}(\bar{X})$ for each objective function

can be specified in a subjective method. Then, for a multi-objective optimization problem with Q objective functions, the final solution can be found as:

$$max\left\{min\left\{\mu_{f_q}(\bar{X})\right\}\right\} \quad ; q = 1,2, \dots Q \quad (43)$$

5. 4. Results

The proposed methodology for optimal locating of TCSC is performed for two cases, as follows:

First case: Optimal locating of TCSC for single-objective congestion management: In this case, total operating cost would be considered as a single objective for optimal placement.

Second case: Optimal locating of TCSC for multi-objective congestion management: In this case, total operating cost, voltage and transient security would be considered as three objectives for optimal placement.

Here, it should be noted that all calculations and analyses are performed for peak load demand and there is more congestion in the network at the same time.

The optimized results for the first case are shown in Table 4. In addition, In order to evaluate the dependability of the proposed method, the results of simulation with modified augmented ε-constraint method [30] are added to Table 4.

Variation of operating cost curve based on the first case using GWO algorithm has been shown in Fig. 7. To solve the problem of sizing TCSC by proposed algorithm,

Table 4. Optimal solution based on the first case

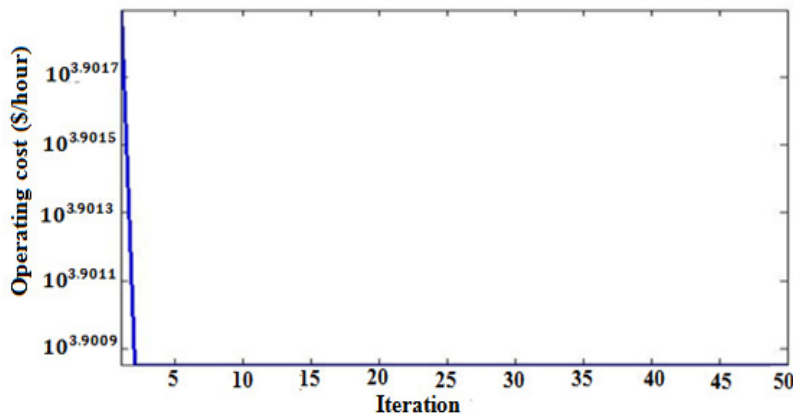|	TCSC branch (Candidate location)	TCSC (%)	Cost ($/hour)
proposed methodology	Line 12: 6-7	70	**7958.89**
Modified augmented ε-constraint method [30]	Line 12: 6-7	70	**7959.69**

Fig. 7. The variation of operating cost curve based on the first case using GWO

GWO algorithm has been run 50 times for this case, and controlling parameter of GWO algorithm is as follow:

Number of grey wolves = 30

The CPU time is needed for sizing TCSC is less than 5 second at each iteration. The evaluation platform is a workstation system with a 2.66 GHZ Intel Core 2 Duo CPU and 4GBs of RAM.

The optimized results for the second case are shown in Table 5. In addition, In order to evaluate the dependability of the proposed method, the results of simulation with modified augmented ε-constraint method [30] are added to Table 5.

The bid curve of generators and benefit curve of demands based on the second case are shown in Fig. 8 and 9, respectively. According to Fig. 8 and 9, the total operating cost (according to Eq. (7)) based on the second case is about US$/hour 10526.

Variation of operating cost curve based on the second case using proposed algorithm has been shown in Fig. 10. The buses voltage magnitude based on the second case has been shown in Fig. 11.

According to Fig. 11, the buses voltage magnitude is increased compared to presence of congestion (without TCSC). The Pareto-approximation fronts (PAFs) achieved from the second case using GWO algorithm is shown in Fig. 12. To solve the problem of sizing TCSC by proposed algorithm, GWO algorithm has been run 50 times for this case, and controlling parameter of GWO algorithm is as follow:

Number of grey wolves= 30

The CPU time is needed for sizing TCSC is less than 20 second at each iteration.

Fig. 12(a)-(c) shows the Pareto-approximation fronts for multi-objective congestion management. Fig. 12(a) shows a relation between the VSM and total operating cost. Increasing the total operating cost, the VSM index is not changed considerably. It is noted that VSM is function of (P_{Dk}, Q_{Dk}). In voltage stability studies, P_{Dk} and Q_{Dk} are usually elevated with a constant power factor by CPF. Therefore, we can say that variables of P_Dk and Q_{Dk} are dependent and thus VSM can be assumed as a

Table 5. Optimal solutions based on the second case

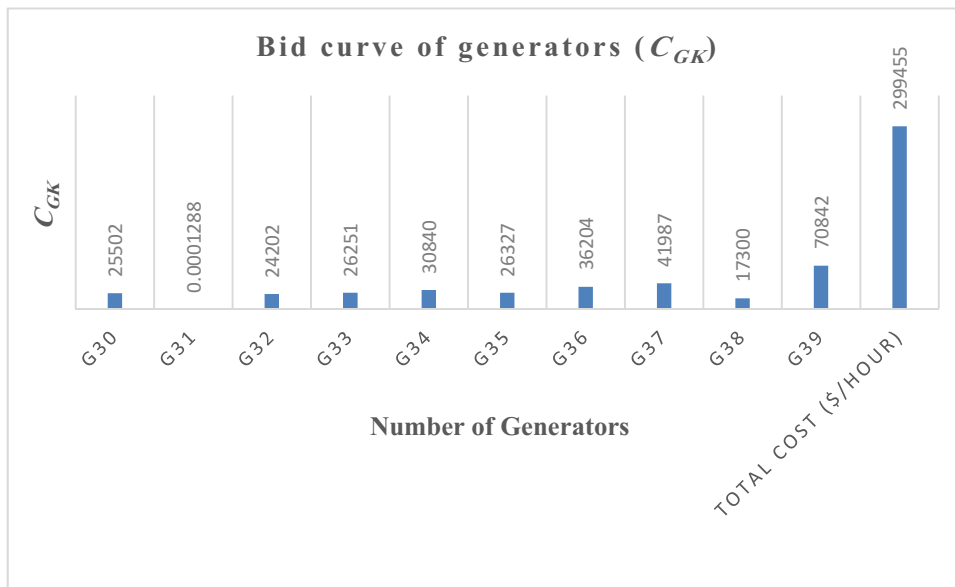|	TCSC branch (Candidate location)	TCSC (%)	Cost ($/hour)	CTEM (per unit)	VSM (%)
proposed methodology	Line 12: 6-7	70	**10526.37**	**43.66**	**40**
Modified augmented -constraint method [30]	Line 12: 6-7	70	**14675.93**	**33.18**	**44.18**

Fig. 8. bid curve of generators based on the second case
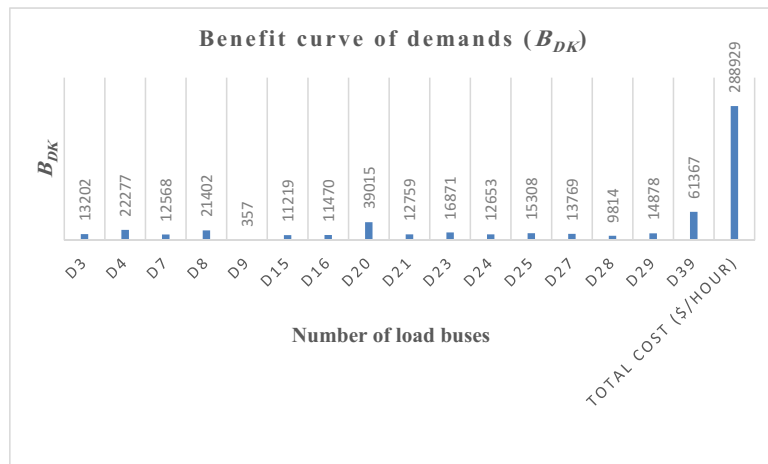
Fig. 9. benefit curve of demands based on the second case
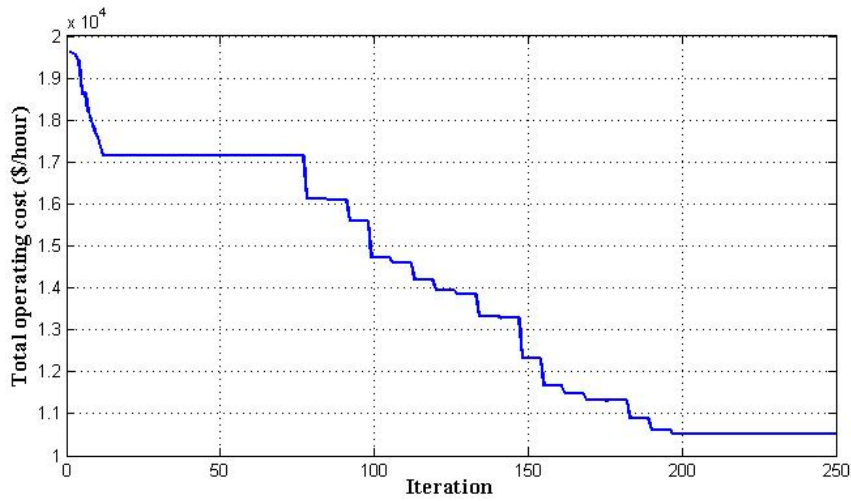

Fig. 10. The variation of operating cost curve based on the second case
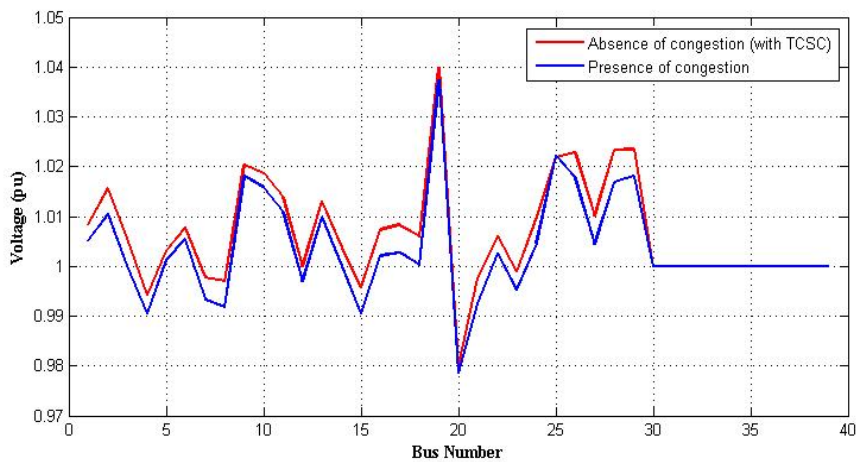

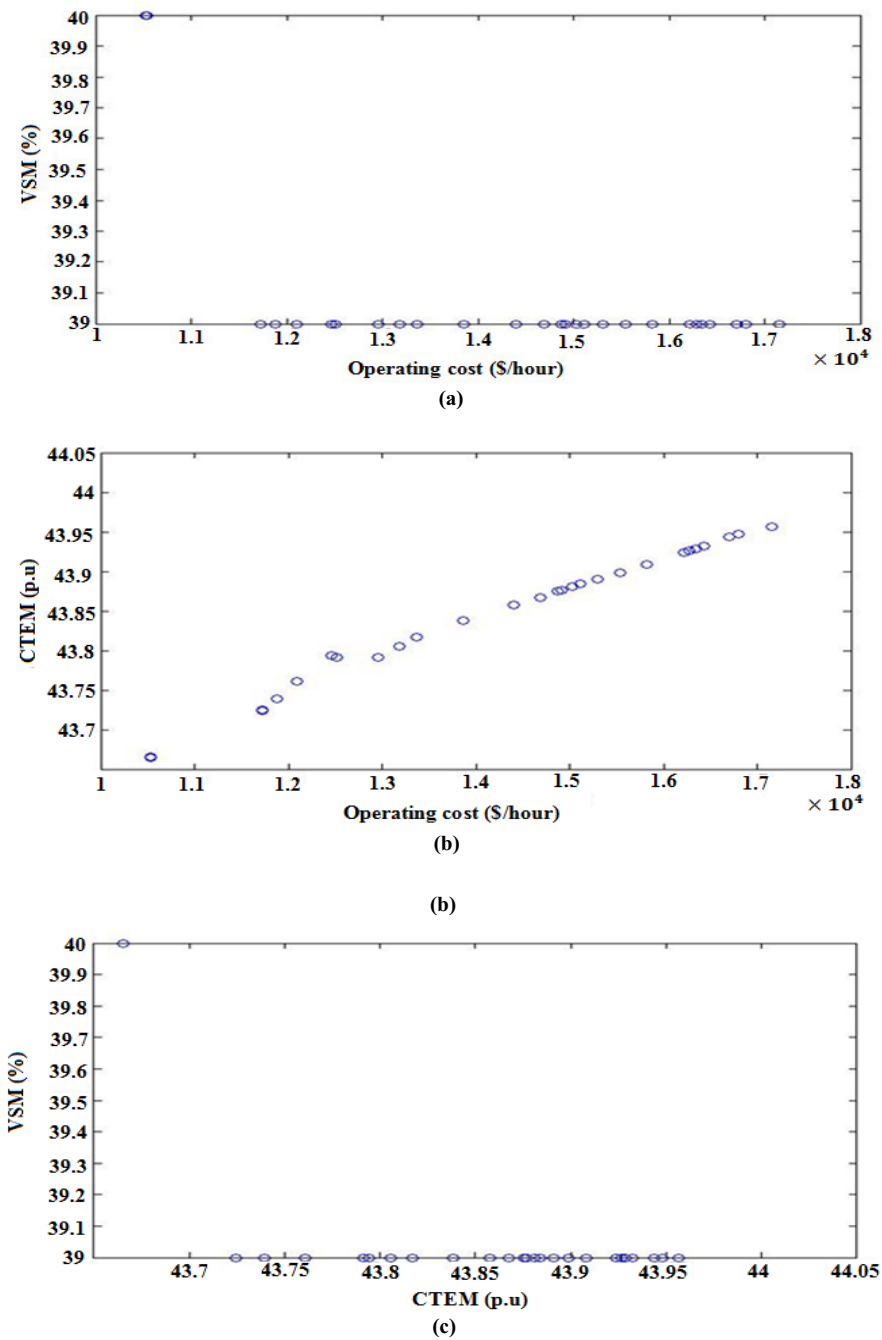**Fig. 11.** Buses voltage magnitude based on the second case

Fig. 12. The PAFs for multi-objective congestion management and trade-offs between (a) VSM and total operating cost. (b) CTEM and total operating cost. (c) VSM and CTEM.

function of only Q_{Dk}, so, by changing the unit's generation and cost, it will not be changes considerably. Fig. 12(b) shows a relation between the CTEM and total operating cost. Increasing the CTEM index increases the total operating cost considerably. When cost is considered as a target, the unit's generation is changed to achieve the minimum cost. On the other hand, when CTEM is considered as a target, due to dependence of CTEM to unit's

generation and difference between unit's generation and optimal value, the cost will be increased. Also, CTEM is function of (P_{Gk}), so, by changing unit's generation and cost, it can be increased. Fig. 12(c) shows a relation between the VSM and CTEM. Increasing the CTEM, the VSM index is not changed considerably.

6. Conclusion

This paper focuses on describing a multi-objective congestion management structure to determine the optimal locating of TCSC. Candidate transmission lines for installation of TCSC are selected by using components of nodal prices. For introducing group of non-dominated solutions, MOGWO algorithm based on OPF is applied. Then fuzzy decision making approach is used to lead to the best response. The results of simulation are compared with other published research papers. The results show that by combining components of nodal prices and grey wolf optimizer, the optimal locating and sizing of the series FACTS devices for multi-objective congestion management can be achieved in restructured power systems by higher convergence speed and more flexibility.

References

[1]. A. Kumar, S. C. Srivastava and S. N. Singh, "Congestion management in competitive Power Systems Research power market: a bibliographical survey", Electric, Vol. 76, pp. 153-164, 2005.

[2]. K. Vijayakumar, "Multiobjective Optimization Methods for Congestion Management in Deregulated Power Systems", Journal of Electrical and Computer Engineering, Vol. 2012, pp. 1-8, 2012.

[3]. S. Verma and V. Mukherjee, "Optimal real power rescheduling of generators for congestion management using a novel ant lion optimiser", IET Generation, Transmission & Distribution, Vol. 10, No. 10, pp. 2548-2561, 2016.

[4]. M. Heydaripour and A. Akbari Foroud, "A New Framework for congestion management with Exact Modeling of Impacting Factors", Iranian Journal of Electrical & Electronic Engineering, Vol. 8, No. 4, pp. 329-340, 2012.

[5]. B. KumarPanigrahi, "Locational Marginal Pricing (LMP) in Deregulated Electricity Market", International Journal of Electronics Signals and Systems, Vol. 1, No. 2, pp. 101-105, 2012.

[6]. N. Acharya and N. Mithulananthan, "Locating series FACTS devices for congestion management in deregulated electricity markets", Electric Power Systems Research, Vol. 77, pp. 352-360, 2007.

[7]. T. Bhattacharjee and A. Kumar Chakraborty, "Congestion management in a deregulated power system by rescheduling of sensitive generators and load curtailment using PSO", International Journal of Emerging Technology and Advanced Engineering, Vol. 2, No. 3, pp. 284-289, 2012.

[8]. N. S. Modi and B. R. Parekh, "Transmission Network Congestion in Deregulated Wholesale Electricity Market", Proceedings of the International Multi Conference of Engineers and Computer Scientists, Hong Kong, Vol. 2, pp. 1-5, 2009.

[9]. E. Eugene Litvinov, T. Zheng, G. Rosenwald and P. Shamsollahi, "Marginal Loss Modeling in LMP Calculation", IEEE Transactions on power systems, Vol. 19, No. 2, pp. 880-888, 2004.

[10]. F. Yong and L. Zuyi, "Different Models and Properties on LMP Calculations", IEEE Power Engineering Society general meeting, Montreal, Que, 2006.

[11]. S. Balaraman and N. Kamaraj, "Real Time Congestion Management in Deregulated Electricity Market Using Artificial Neural Network", Iranian Journal of Electrical and Computer Engineering, Vol. 10, No. 1, pp. 34-40, 2011.

[12]. K. Singh, N. P. Padhy and J. Sharma, "Congestion management considering hydro-thermal combined operation in a pool based electricity market", Electrical Power and Energy Systems, Vol. 33, pp. 1513-1519, 2011.

[13]. S. A. Hosseini, N. Amjady and M. Shafie-khah, "A new multi-objective solution approach to solve transmission congestion management problem of energy markets", Applied Energy, Vol. 165, pp. 462-471, 2016.

[14]. H. Patel and R. Paliwal, "Congestion management in deregulated power system using facts devices", International Journal of Advances in Engineering & Technology, Vol. 8, No. 2, pp. 175-184, 2015.

[15]. M. Gitizadeh and M. Kalantar, "FACTS devices allocation to congestion alleviation incorporating voltage dependence of loads", Iranian Journal of Electrical & Electronic Engineering, Vol. 4, No. 4, pp. 176-190, 2008.

[16]. N. R. Kumari and K. C. Sekhar, "Optimal Placement of TCSC Based on Sensitivity Analysis for Congestion Management", International Journal of Electrical and Computer Engineering (IJECE), Vol. 6, No. 5, pp. 2041-2047, 2016.

[17]. K. Arun Kumar Reddy and P. S. Shiv, "Congestion mitigation using UPFC", IET Generation, Transmission & Distribution, Vol. 10, No. 10, pp. 2433-2442, 2016.

[18]. A. Mishra and V. N. Kumar Gundavarapu, "Line utilisation factor-based optimal allocation of IPFC and sizing using fire fly algorithm for congestion management", IET Generation, Transmission & Distribution, Vol. 10, No. 1, pp. 115-122, 2016.

[19]. R. Jahani, H. ChahkandiNejad, A. ShafighiMalekshah and H. A. Shayanfar, "A New Advanced Heuristic Method for Optimal Placement of Unified Power Flow Controllers in Electrical Power Systems", Int. Rev. Electr. Eng. (IREE), Vol. 5, No. 6, pp. 2786-2794, 2001.

[20]. A. Kumar and C. Sekhar, "Comparison of Sen Transformer and UPFC for congestion management in hybrid electricity markets", International Journal of Electrical Power & Energy Systems, Vol. 47, pp. 295-304, 2013.

[21]. A. LashkarAra, J. Aghaei and M. Shabani, "Introducing a Fuzzy Interactive Multi-objective Approach to Optimal Location of UPFC", Int. Rev. Electr. Eng. (IREE), Vol. 5, No. 6, pp. 2896-2906, 2010.

[22]. B. Bhattacharyya and V. K. Gupta, "Fuzzy Genetic Algorithm Approach for the Optimal Placement of Flexible AC Transmission Systems Devices in a Power System", Electric Power Components and Systems, Vol. 42, No. 8, pp. 779-787, 2014.

[23]. A. Y. Abdelaziz, M. A. El-Sharkawy and M. A. Attia, "Optimal location of thyristor-controlled series compensators in power systems for increasing loadability by genetic algorithm", Electric Power Components and Systems, Vol. 39, pp. 1373-1387, 2011.

[24]. R. A. Hooshmand, M. J. Morshed and M. Parastegari, "Congestion management by determining optimal location of series FACTS devices using hybrid bacterial foraging and Nelder-Mead algorithm", Applied Soft Computing, Vol. 28, pp. 57-68, 2015.

[25]. A. Zamora-Cárdenas and C. R. Fuerte-Esquivel, "Multi-parameter trajectory sensitivity approach for location of series-connected controllers to enhance power system transient stability", Electric Power Systems Research, Vol. 80, pp. 1096-1103, 2010.

[26]. S. R. Inkollu and V. R. Kota, "Optimal setting of FACTS devices for voltage stability improvement using PSO adaptive GSA hybrid algorithm", International Journal Engineering Science and Technology, Vol. 19, No. 3, pp. 1166-1176, 2016.

[27]. N. Amjady and M. Esmaili, "Improving voltage security assessment and ranking vulnerable buses with consideration of power system limits", International Journal of Electrical Power & Energy Systems, Vol. 25, pp. 705-715, 2003.

[28]. F. Da-Zhong, T. S. Chung, Z. Yao and S. Wennan, "Transient stability limit conditions analysis using a corrected transient energy function approach", IEEE Transactions on Power Systems, Vol. 15, pp. 804-810, 2000.

[29]. P. Kumar Tiwari and Y. Raj Sood, "An Approach for Optimal Placement, Rating and Investment Cost Recovery of a TCSC in Double Auction Power Market", Proceedings of International Conference on Power Systems, Energy, Environment, pp. 91-97, 2014.

[30]. M. Esmaili, H. A. Shayanfar and R. Moslemi, "Locating series FACTS devices for multi-objective congestion management improving voltage and transient stability", European Journal of Operational Research, Vol. 236, pp. 763-773, 2014.

[31]. L. Chen, H. Suzuki, T. Wachi and Y. Shimura, "Components of Nodal Prices for Electric Power Systems", IEEE Trans. Power Apparat. Syst., Vol. 17, No. 1, pp. 41-49, 2002.

[32]. S. Mirjalili, S. Saremi., S. M. Mirjalili and L. Coelho, "Multi-objective grey wolf optimizer: A novel algorithm for multi-criterion optimization", Expert Systems with Applications, Vol. 47, pp. 106-119, 2016.

[33]. P. Maghouli, S. H. Hosseini, M. Buygi and M. Shahidepour, "A multi-objective framework for transmission expansion planning in deregulated environments", IEEE Trans. on Power Syst., Vol. 24, No. 2, pp. 1051-1061, 2009.

Alireza Moradi was born in Semnan, Iran, in 1986. He received the B.Sc. and M.Sc. degrees in electrical engineering from Semnan and Birjand University in 2010 and 2012, respectively. He is currently a Ph.D. student at the Semnan University. His research interests include security assessment of power systems, power system planning, power quality, artificial intelligence, and its application to the problems of the power systems.

Yousef Alinejad-Beromi was born in Damghan, Iran. He received the B.Sc. degree in electrical engineering from K.N.T. University, Tehran, Iran, and the M.Sc. and Ph.D. degrees from UWCC, Cardiff, U.K., in 1989 and 1992, respectively. He is currently an Associate Professor with the Faculty of Electrical and Computer Engineering, Semnan University, Semnan, Iran.

Kourosh Kiani was born in Semnan, Iran. He received the B.Sc. and M.Sc., degrees in electrical engineering from Delft University of Technology in Delft, the Netherlands in 1993 and the Ph.D. degree in Medical information from Erasmus University in Rotterdam, the Netherlands in 1997. He is currently an Assistant Professor with the Faculty of Electrical and Computer Engineering, Semnan University, Semnan, Iran. His research interests include artificial intelligence, neural network, and fuzzy logic.